Asian J. Exp. Sci., Vol. 22, No. 2, 2008; 63-74

Friction Stir Welding of Al 6061 Alloy

N. T. Kumbhar and K. Bhanumurthy*
Materials Science Division
Bhabha Atomic Research Centre
Trombay, Mumbai - 400085. India

Abstract : Friction stir welding, a solid state joining technique, is widely being used for joining Al alloys for aerospace, marine automotive and many other applications of commercial importance. FSW trials were carried out using a vertical milling machine on Al 6061 alloy. The tool geometry was carefully chosen and fabricated to have a nearly flat welded interface. Important process parameters that control the quality of the weld are a) axial force b) rotation speed (rpm) c) traverse speed (mm/min) and d) tool tilt angle and these process parameters were optimized to obtain defect free welded joints. It is observed that, during the friction stir welding, extensive deformation is experienced at the nugget zone and the evolved microstructure strongly affects the mechanical properties of the joint. The present studies aimed to understand the microstructural changes and the associated mechanical properties during the FSW and also after post weld heat treatment (PWHT). The resultant microstructure was characterized using electron probe microanalysis (EPMA), secondary electron microscopy (SEM) and orientation imaging microscopy (OIM). This paper presents the optimization of process parameters and also highlights the influence of PWHT on the microstructure, composition variation across the interface and mechanical properties of FSW 6061 Al alloy

Keywords: Friction stir welding, Al 6061 alloy, microstructure, mechanical properties, recrystallization.

Introduction

Friction stir welding, a solid state joining technique invented in 1991 by The Welding Institute (TWI) (Thomas *et al*. 1992), is extensively used in the joining of Al, Mg, Cu, Ti and their alloys (Liu *et al*., 1997; Krishnan, 2002a, 2002b; Lee *et al*., 2003, 2004,2005;Rhodes *et al*., 1997; Sato *et al*., 2004a, 2004b; Srivatsan *et al*., 2007). This technique has been extended to dissimilar welding of the above-mentioned alloys and also to the welding of steels.(Somasekharan and Murr, 2004; Fujii *et al*., 2006; Watanabe *et al*., 2006; Lee *et al*., 2006)

The process of Friction Stir Welding has been widely used in the aerospace, shipbuilding, automobile industries and in many applications of commercial importance. This is because of many of its advantages over the conventional welding techniques some of which include very low distortion, no fumes, porosity or spatter, no consumables (no filler wire), no special surface treatment and no shielding gas requirements. FSW joints have improved mechanical properties and are free from porosity or blowholes compared to conventionally welded materials. However along with these advantages there are a few disadvantages, which also need to be mentioned. At the end of the welding process an exit hole is left behind when the tool is withdrawn which is undesired in most of the applications. This has been overcome by providing an offset in the path for continuous trajectory, or by continuing into a dummy plate for non-continuous paths, or simply by

machining off the undesired part with the hole. Large down forces and rigid clamping of the plates to be welded are a necessity for this process, which causes limitation in the applicability of this process to weld jobs with certain geometries.

In FSW, a cylindrical-shouldered tool, with a profiled threaded/unthreaded probe or pin is rotated at a constant speed and fed at a constant traverse rate into the joint line between two pieces of sheet or plate material, which are butted together as shown in Figure 1. The parts have to be clamped rigidly onto a backing bar in a manner that prevents the abutting joint faces from being forced apart. The length of the pin is slightly less than the weld depth required and the tool shoulder should be in intimate contact with the work piece surface. The pin is then moved against the work piece, or vice-versa.

Frictional heat is generated between the wear resistant welding tool shoulder and pin, and the material of the work-pieces. This heat, along with the heat generated by the mechanical mixing process and the adiabatic heat within the material, cause the stirred materials to soften without reaching the melting point (hence cited a solid-state process). As the pin is moved in the direction of welding the leading face of the pin, assisted by a special pin profile, forces plasticized material to the back of the pin whilst applying a substantial forging force to consolidate the weld metal. The welding of the material is facilitated by severe plastic deformation in the solid state involving dynamic recrystallization of the base material.

Friction Stir Welding is associated with various types of defects (Chen *et al*., 2006; Kim *et al*., 2006) which result due to

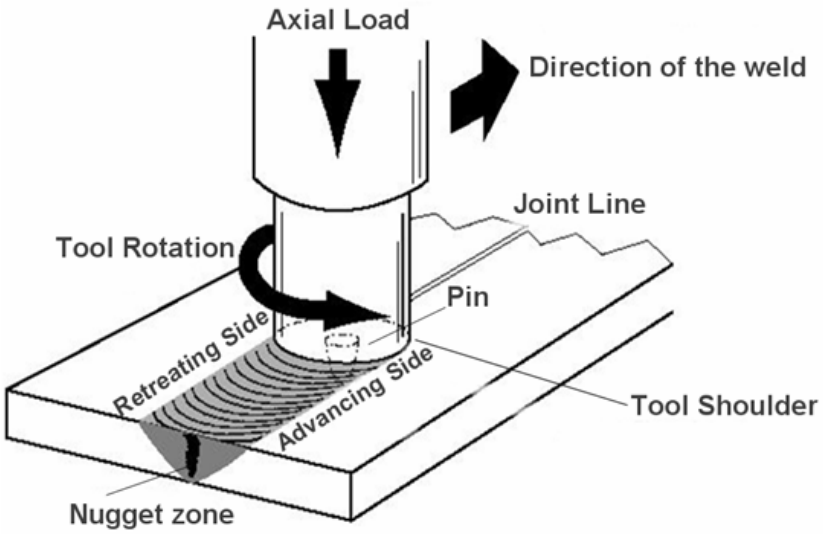

Fig. 1 : Schematic of Friction Stir Welding.

improper welding parameters. Insufficient weld temperatures, due to low rotation speeds or high traverse speeds, for example, mean that the weld material is unable to accommodate the extensive deformation during welding. This may result in long, tunnel defects running along the weld which may be surface or subsurface. Low temperatures may also limit the forging action of the tool and so reduce the continuity of the bond between the materials from each side of the weld. The light contact between the materials has given rise to the name 'kissing-bond'. This defect is particularly worrying since it is very difficult to detect using non-destructive methods such as X-ray or ultrasonic testing. If the pin is not long enough or the tool rises out the plate then the interface at the bottom of the weld may not be disrupted and forged by the tool resulting in a lack-of-penetration defect. This is essentially a notch in the material which can be a potent source of fatigue cracks.

Extensive literature of friction stir welding of Al alloys does indicate that there are few areas particularly on the correlation of microstructure with the mechanical properties for 6061 Al alloy needed further investigation. The present work aims to understand the process mechanism of friction stir welding, the evolution of the microstructure as a result of these processes and also determines the mechanical properties of the welded joints.

Methods and Materials

Materials : Partially recrystallized AA 6061 having the chemical composition 0.92 Mg-0.6 Si-0.33 Fe-0.2 Ca-0.18 Cu-0.06 Mn-0.03 Zn-0.02 Ti-(Al balance) was used. The dimensions of the 6061 Al plates were 300 mm x 50 mm x 5 mm. A high-speed steel tool was used for welding 6061 Al alloy having the shoulder diameter of 25 mm. The tool had a pin height of 4.8 mm and a 5 mm pin diameter.

Welding Parameters : The 6061 Al plates were welded using three different tool rotation speeds and tool traverse speeds. The tool rotation speeds used in this study were 710, 1120 and 1400 rpm and the tool traverse speeds of 63, 80 and 100 mm/min were used. The tool tilt in all the trials was kept constant at 2°.

Method : The friction stir welded plates were taken for non-destructive evaluation comprising of the die penetration test and X-ray radiography. Only those sample plates that qualified in the aforementioned tests were taken for detailed microstructural characterization. For the optical microscopy the samples were cut in a direction perpendicular to the welding direction. Some of these samples were given a post weld heat treatment schedule consisting of solutionizing at 530ºC for 30 min and then aged at 160ºC for different periods of 4, 8, 12 and 18 hrs. These samples were then grinded successively on SiC papers of grit 220 to 600. After which they were polished on a fine cloth using a 1µm diamond paste to obtain a mirror finish. The samples were then etched using a solution of 10 ml HF + 15 ml HCl + 25 ml HNO_3 + 50 ml H_2O. These were then used for optical microscopy, EPMA and SEM analysis. The metallographically polished samples to be used for OIM were further electrolytically polished in a solution of 80 % methanol and 20 % perchloric acid at –20ºC and at 11 V.

The microhardness measurements were taken on the cross section perpendicular to the welding direction using an indentor with a load of 50 gf for a dwell period of 10 s.

To evaluate the mechanical properties standard tensile specimens were fabricated in a direction perpendicular to the welding direction having a gauge length of 25 mm. These were then tested on a screw driven Instron Machine at strain rates of 10^{-3} sec^{-1}. The fractured surfaces were examined using an SEM.

Results and Discussion

Based on detailed experimental study a process map was obtained for optimizing the process parameters. All these specimens which passed both the die penetration test and X-ray radiography tests were designated as 'defect free' and those who did not qualify the tests as 'defective' for a given set of process parameters (rpm, mm/min). Figure 2 shows the process map obtained based on the present experimental work for Al 6061-O condition and also for comparison of these process parameters, some of the values taken from the work of Lim *et al*. (2004) for Al 6061-T651 are also shown. In Figure 2 the unfilled symbols O, Δ stand for the values obtained from the present study, with the corresponding X and Y axes on the bottom and left of the plot respectively whereas the filled symbols ●, ▲ refer to the values taken from the work of Lim *et al*. (2004) with corresponding X and Y axes on the top and the right of the plot respectively.

It can be seen from Figure 2 that FSW of 6061 Al alloy in the solutionized condition has specific advantages. Defect free joints could be obtained for lower rotation speed 700 rpm and with a high feed rate of 80 mm/min. On the other hand it is essential to have

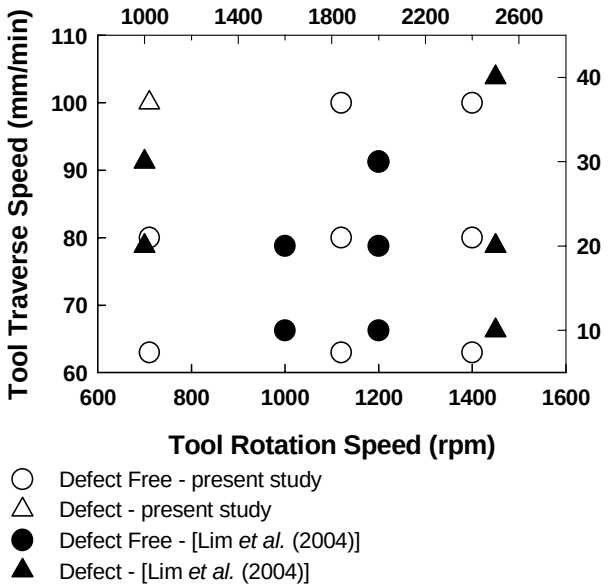

Fig. 2 : Process map for Al 6061-O in comparison with the work by Lim *et al*. (2004) for Al 6061-T651.

a minimum of 1000 rpm for Al 6061-T651 condition to obtain similar welding speeds. The specific advantage of using this alloy in O-condition is its lower hardness (38 VHN). It is possible to stir this alloy at lower rotation speeds and at higher welding speeds. Better mechanical properties for these joints can be obtained by subjecting these to post weld heat treatment such as the T6 condition.

Digital low magnification image for the specimen welded at a rotation speed of 1400 rpm and feed of 80 mm/min is shown in Figure 3(f). Figure 3(a)-(d) show the microstructures in the regions marked (a)-(d) in Figure 3(f) corresponding to the base metal, advancing side interface, nugget and retreating side interface respectively. Figure 3(c) and (e) are back-scattered electron (BSE) images showing the microstructure in the nugget zone for the as welded and post weld heat treated (PWHT) specimens respectively. It is clear from these micrographs that the welded region is free from defects. Based on the detailed metallographic studies, three regions could be identified as i) parent material ii) thermo-mechanical and heat affected zone (TMAZ) and iii) nugget zone (NZ) and these regions are marked as a, b and c in Figure 3(f). This distinction is based upon the changes in the resultant microstructure as an effect of the deformation induced and the frictional heat produced by the stirring tool and also the precipitate distribution in the corresponding regions. The parent material consists of elongated grains having a grain size in the range -100 μm. The nugget consists of fine equiaxed grains an order less in magnitude to that of the parent material ranging between 15-20 μm. The thermomechanically affected zone (TMAZ) consists of grains having similar size as that of the parent material with a modified bent morphology which is due to the induced deformation of the region adjacent to the nugget as a result of the stirring action of the rotating tool and the consequent frictional heat produced. There is no significant change observed in the microstructure of the heat affected zone (HAZ) when compared with that of the parent material albeit the precipitate distribution being different in these two regions. The small grain size in the nugget zone is due to the stirring action of the tool which induces high amount of plastic deformation and the frictional heat generated between the tool and the workpieces. This process of formation of smaller grain size in the nugget zone is based on the mechanism of continuous dynamic recrystallization.

Figure 4 shows the microhardness profile taken across the weld zone, along the line PQ as shown in Figure 3f, for both the as welded specimen and the post weld heat treated specimen. For the as weld specimen the profile indicates a higher hardness in the nugget region (65-70 VHN) compared to the base material (37-42 VHN). This is because the as received parent material was in the homogenized condition wherein all the precipitates are dissolved, thus accounting to a lower hardness due to the absence of strengthening precipitates. In the nugget region, which experiences higher temperatures than the remaining regions, the dissolved precipitates do reprecipitate subsequently. Here the precipitates are finer and uniformly distributed in the nugget region. The microhardness values for the PWHT specimen show no such characteristic distribution and is more or less uniform throughout. The microhardness values of the solutionized parent material and those of the parent material in the T6 temper are shown by horizontal dotted and continuous lines respectively for comparison.

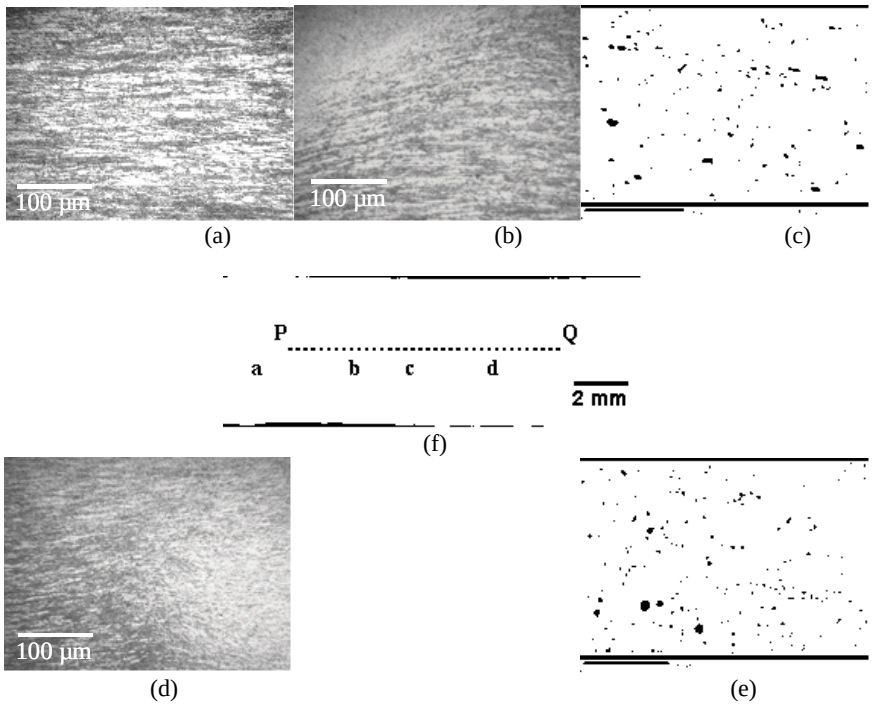

Fig. 3 : Microstructures of FSW 6061 Al alloy at the (a) matrix, (b) advancing side interface, (c) nugget and (d) retreating side interface for the as welded specimen, (e) nugget for PWHT specimen and (f) the digital micrograph of as welded specimen showing the locations of above micrographs

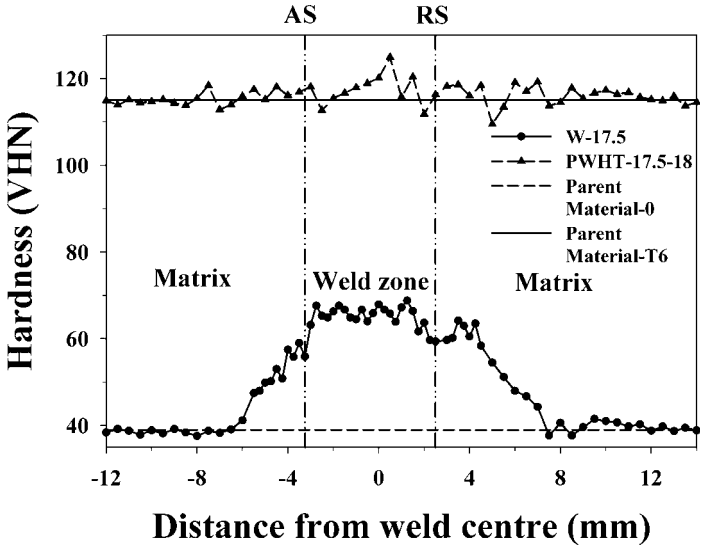

Fig. 4 : Microhardness plot taken along line PQ (as shown in Fig. 3f)

X-ray line scans of O ($K_{á}$), Mg ($K_{á}$), Si ($K_{á}$) and Al ($K_{á}$) taken from top to about 60 ìm (perpendicular to line PQ as shown in Figure 3f) inside the weld pool for as welded and PWHT specimen (which was aged for 18 hrs) are shown in Figure 5(a) and (b) respectively. Care was taken to avoid the flash regions of the stirred zone. The initial zero intensities for all the elements correspond to the cold set resin material used for mounting the sample. There is oxygen pickup up to a depth of about 20 ìm and this resulted in the change in the local chemical composition of the alloying elements Mg and Si. Recent studies on FSW of 6111 Al alloy show that the highest temperature reached during welding is close to 0.94 T_s (Park *et al*., 2004) where T_s is the solidus temperature of the alloy in K. Assuming similar relation in the present studies, the temperature of 530°C could have been seen at the top of the weld, resulting in pickup of oxygen from the surroundings and the local compositional change.

Typical composition profiles taken along the line PQ for the as welded specimen and the PWHT specimen showed that the distribution of Al, Mg and Si for both these specimens is nearly uniform. Though there is certain degree of inhomogenity in terms of grain size in the nugget zone, there is practically a high degree of chemical homogeneity in the stirred region. The discontinuities observed in the concentration profiles indicate the formation of intermetallics. Two types of intermetallics i) aluminum rich Al_xSi_y(Fe) and ii) magnesium rich Mg_xSi_y(Al) could be identified from these profiles. It is observed that the size of these precipitates in the nugget zone is small compared to those found in the matrix and this reduction possibly could be due to the stirring action of the tool.

Figure 6. shows the orientation imaging microscopy (OIM) scans in the base material, advancing side, nugget and the retreating side at the regions represented by points a, b, c and d as shown in Figure 3f. The base material (Figure 6a) shows elongated pancake shaped grains of the magnitude of 100 µm. The base material is textured as is readily seen from the OIM scan. The nugget (Figure 6c) shows equiaxed grains having random orientation and an average grain size of 10 ìm. Figure 6b shows that at the advancing side a morphological bending of the grains can be seen at the interface near the nugget. Whereas on the retreating side (Figure 6d) no such clear switch is seen.

Table I lists the mechanical properties of all the welded specimens for various combinations of rotation speeds and welding speeds. In the chosen narrow window of process parameters, the values of UTS and elongation (%) do not vary significantly. All the specimens failed away from the nugget zone. The UTS values for the welded specimens are much larger compared to the parent material at O-condition (P-O). The maximum elongation value for the welded specimens is around 18 % and this value is about 25 % less than the parent material. In order to study the behavior of mechanical properties on ageing, the specimens processed with rotation speed 1400 rpm and welding speed 80 mm/min were taken for PWHT for different duration. The mechanical properties of these PWHT specimen aged at different duration are shown in Table II. It can be seen that specimens aged for 4 hrs show superior mechanical properties

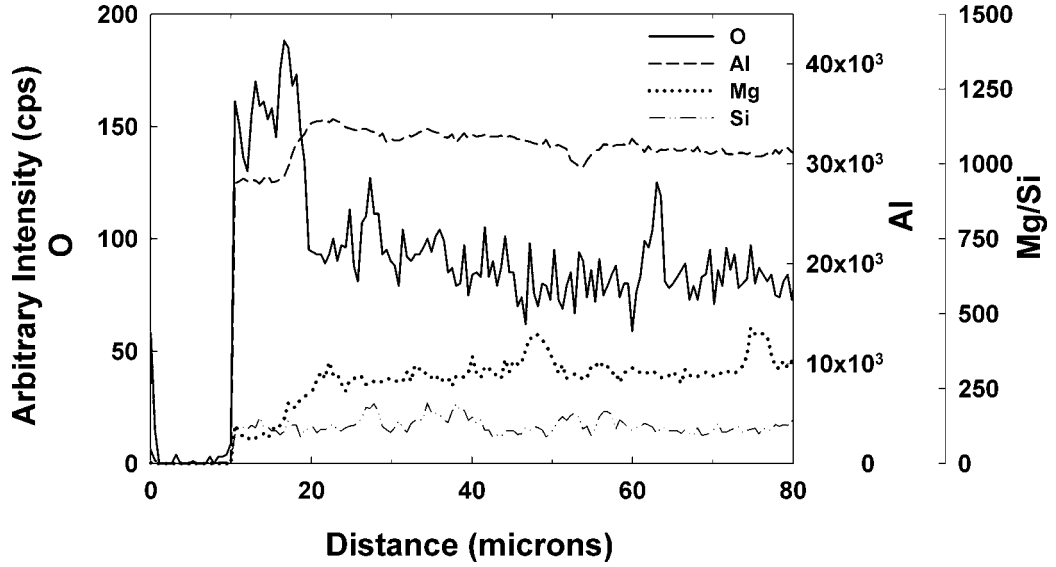

(a)

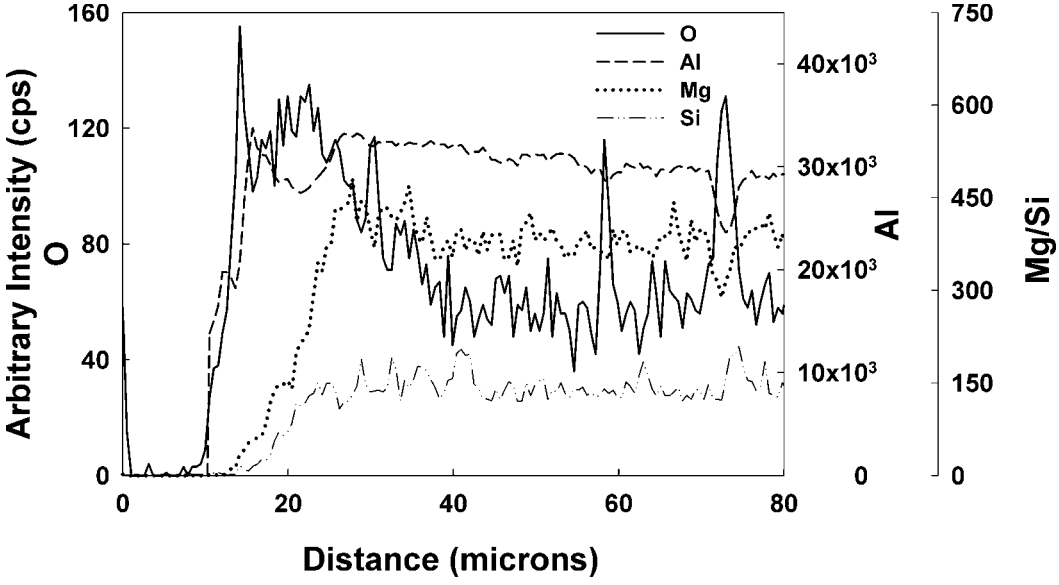

(b)

Fig. 5 : (a), (b) Line scan of O (K_{α}), Mg (K_{α}), Si (K_{α}) and Al (K_{α}) taken perpendicular to the line PQ (Fig. 3f) from top to about 60 ìm for as welded and PWHT-17.5-18 specimens.

Table I : Comparison of Ultimate Tensile Strength (UTS), Yield Strength (YS) and % elongation for as welded specimens for various combinations of tool rotation speeds and tool traverse speeds.

	Tool Rotation Speed (rpm)	Tool Traverse Speed (mm/min)	UTS (MPa)	YS (MPa)	Elongation (%)
1	710	63	164.8	74.2	18.7
2	710	80	155	70.5	12.2
3	1120	63	159.6	75.4	16
4	1120	80	162	80	15.4
5	1120	100	160	73.8	14.8
6	1400	63	155	70.5	12.2
7	1400	80	159.6	75.4	16
8	1400	100	162	80	15.4
9					
10					

Table II : Comparison of Ultimate Tensile Strength (UTS), Yield Strength (YS) and % elongation for specimens welded at tool rotation speed of 1400 rpm and tool traverse speed of 80 mm/min for different aging periods.

Aging Time (hrs)	UTS (MPa)	YS (MPa)	Elongation (%)
1	164.8	74.2	18.7
4	155	70.5	12.2
8	159.6	75.4	16
12	162	80	15.4
T6 condition	310	275	12
O - condition	125	55	24

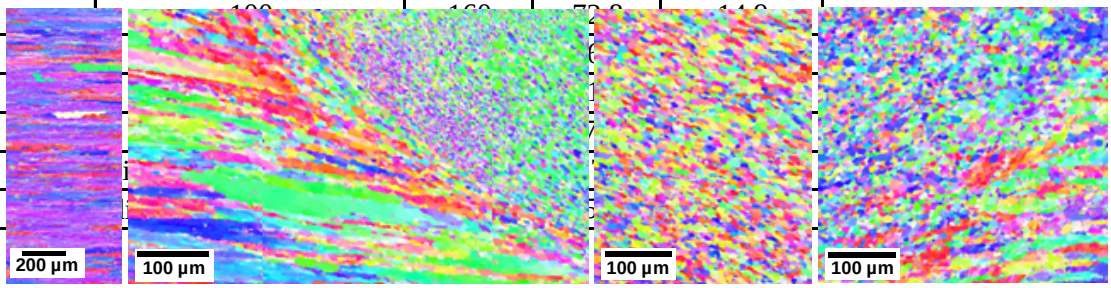

Fig. 6 : The Orientation Imaging Microscopy (OIM) scans taken in the (i) base material, (ii) advancing side, (iii) nugget and (iv) retreating side at positions a, b, c and d respectively as shown in Fig. 3f.

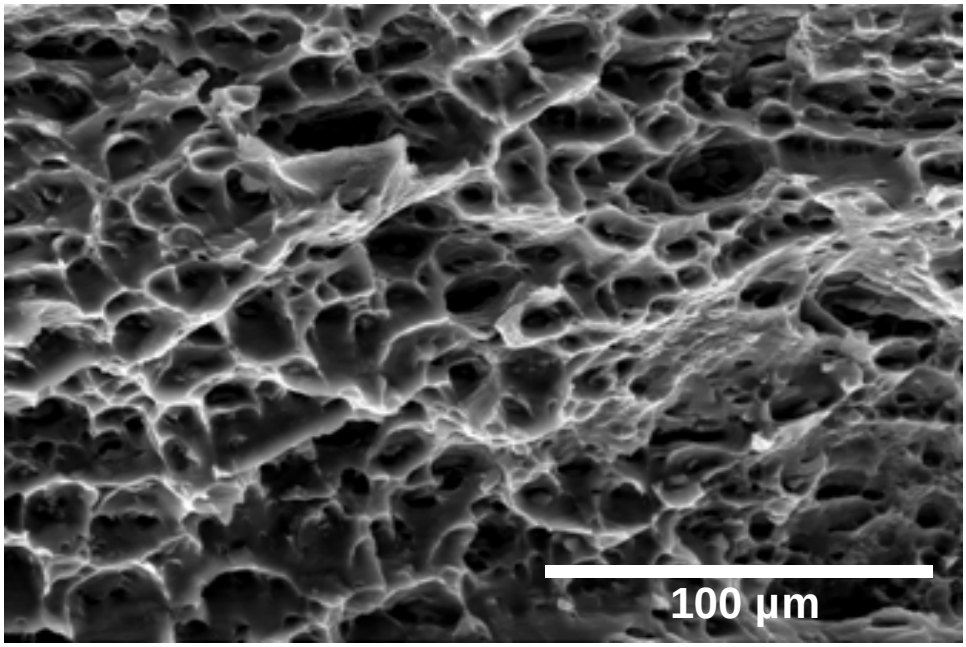

Fig. 7 : Fractograph image for PWHT-17.5 specimen aged for 18 hrs.

compared to those of the parent material and these specimens also failed away from the weld zone. It is clearly seen that ageing for duration of 1, 4 and 8 hrs restores the strength comparable to that of the parent material in the T6 condition (P-T6), without any significant loss in the ductility. These superior mechanical properties after PWHT could be due to homogeneous distribution of precipitates in the weld zone (Park *et al.*, 2004). However aging for longer duration does bring down the strength and ductility as expected due to the coarsening of the precipitates.

Normally FSW of most of the aluminum alloys are carried out in the aged condition (T6 condition). This always requires higher tool forces and optimization of process parameters needs larger window. In addition, during welding softening takes place in the nugget zone resulting in poor mechanical properties (Liu *et al.*, 2003; Lee *et al.*, 2005). In order to restore all the mechanical properties, generally PWHT in T6 condition may be required. The present studies suggest that experiments carried out under O-condition have specific advantages of FSW in a narrow window and at lower rotation feeds. Further, PWHT may be carried out to restore most of the mechanical properties.

Fracture of the as welded and also PWHT specimens mostly occurred on the retreating side and at the lowest hardness values. A few as-welded specimens at rotation feed of 22 rotations/mm failed at the advancing side. The fractographs taken at nearly same magnification for specimen welded at process parameters of 1400 rpm and 80 mm/min and aged at 18 hrs is shown in Figure 7. All PWHT specimens showed

superior mechanical properties and the fractured surfaces show the presence of fine dimple structures, a clear evidence of ductile mode of fracture (Figure 7).

Conclusions

Aluminium alloys 6061 and was successfully welded. A process window of optimized parameters for the Al 6061-O condition was generated and it was observed that using the parent material in the O-condition it is useful to fiction stir weld at lower tool rotation speeds and at a higher welding speed, thus enhancing the productivity. Friction stir welding of Al 6061-O condition, increases the strength of the weld joint as compared to that of the parent material in O-condition at the cost of the ductility, for all welding trials. But the ductility is equal to or better than that of the parent material in T6 condition. Moreover PWHT upto 8 hours restore the strength and ductility of the weld joint comparable to that of the parent material in T6 condition. Microstructural inhomogeneity exists in the FSW specimens. PWHT substantially reduces these inhomogenities. In general FSW does not result in chemical inhomogeneity in a scale of 1 ìm. There is oxygen pickup resulting in the change of local chemical composition of the alloying elements at the surface. Orientation imaging microscopy results suggest that the base material is more textured than the nugget region. The nugget has grain size of around 10 ìm. At the advancing side interface, the grains of the base material show a morphological bending whereas no such characteristic is observed on the retreating side interface. This explains the characteristic sharpness of the advancing side interface than the rather diffuse retreating side interface. FSW on the O-condition has specific advantages in terms of optimizing the process parameters. Mechanical properties substantially improve during PWHT and at an optimized heat treatment schedule. Fracture mostly occurred on the retreating side and the fracture surface show dimple structure.

References

Chen H. B., Yan K., Lin T., Chen S. B., Jiang C. Y. and Zhao, Y. (2006) : The investigation of typical welding defects for 5456 aluminum alloy friction stir welds, *Materials Science and Engineering*, **433A**, 64-69.

Fujii H., Cui L., Tsuji N., Maeda M., Nakata K. and Nogi K. (2006) : Friction stir welding of carbon steels, *Materials Science and Engineering*, **429A**, 50-57.

Kim Y. G., Fujii H., Tsumura T., Komazaki T. and Nakata K. (2006) : Three defect types in friction stir welding of aluminum die casting alloy, *Materials Science and Engineering*, **415A**, 250-254

Krishnan K. N. (2002a) : On the formation of onion rings in friction stir welds, *Materials Science and Engineering*, **327A**, 246-251.

Krishnan K. N. (2002b) : The effect of post weld heat treatment on the properties of 6061 friction stir welded joints, *Journal of Materials Science*, **37**, 473-480.

Lee W. B., Yeon Y. M. and Jung S. B. (2003) : Joint properties of friction stir welded AZ31B - H24 magnesium alloy, *Materials Science and Technology*, **19**, 785-790.

Lee W. B. and Jung S. B. (2004) : The joint properties of copper by friction stir welding, *Materials Letters*, **58**, 1041-1046.

Lee W. B., Lee C. Y., Chang W. S., Yeon Y. M. and Jung S. B. (2005) : Microstructural investigation of friction stir welded pure titanium, *Materials Letters*, **59**, 3315-3318.

Lee W. B., Schmuecker M., Mercardo U. A., Biallas G. and Jung S. B. (2006) : Interfacial reaction in steel-aluminum joints made by friction stir welding, *Scripta Materialia*, **55**, 355-358.

Lim S., Kim S., Lee C. G. and Kim S. (2004) : Tensile behavior of friction-stir-welded Al 6061-T651, *Metallurgical and Materials Transactions*, **35A**, 2829-2835.

Liu G., Murr L.E., Niou C. S., McClure J. C. and Vega F. R.(1997) : Microstructural aspects of the friction-stir welding of 6061-T6 aluminum, *Scripta Materialia*, **37**, 355-361.

Liu H., Fujii H., Maeda M. and Nogi K. (2003) : Tensile properties and fracture locations of friction-stir welded joints of 6061-T6 aluminum alloy, *Journal of Material Science Letters*, **22**, 1061-1063.

Park H. S., Kimura T., Murakami T., Nagano Y., Nakata K. and Ushio M. (2004) : Microstructures and mechanical properties of friction stir welds of 60% Cu-40% Zn copper alloy, *Materials Science and Engineering*, **371A**, 160-169.

Sato Y. S., Sugiura Y., Shoji Y., Park S. H. C., Kokawa H. and Ikeda K. (2004a) : Post-weld formability of friction stir welded Al alloy 5052, *Materials Science and Engineering*, **369A**, 138-143.

Sato Y. S., Yamashita F., Sugiura Y., Park S. H. C. and Kokawa H. (2004b) : FIB-assisted TEM study of an oxide array in the root of a friction stir welded aluminium alloy, *Scripta Materialia*, **50**, 365-369.

Somasekharan A. C. and Murr L. E. (2004) : Microstructures in friction-stir welded dissimilar magnesium alloys and magnesium alloys to 6061-T6 aluminum alloy, *Materials Characterization*, **52**, 49- 64.

Srivatsan T. S., Vasudevan S. and Park L. (2007) : The tensile deformation and fracture behavior of Friction Stir Welded aluminum alloy 2024, *Materials Science and Engineering*, **466A**, 235-245.

Thomas W. M., Nicholas E. D., Needham J. C. and Murch M. G. (1992) : Improvements relating to friction welding, European Patent EP 0615480 B1

Watanabe T., Takayama H. and Yanagisawa A. (2006) : Joining of aluminum alloy to steel by friction stir welding, *Journal of Materials Processing and Technology*, **172**, 342-349.